A new critical velocity in the dynamic fracture of brittle amorphous materials

Julien Scheibert, Claudia Guerra, Fabrice Célarié, Davy Dalmas, Daniel Bonamy

A new critical velocity in the dynamic fracture of brittle amorphous materials

J. Scheibert,[1,2,*] C. Guerra,[1,3] F. Célarié,[1,2,†] D. Dalmas,[2] and D. Bonamy[1]

[1] *CEA, IRAMIS, SPCSI, Grp. Complex Systems & Fracture, F-91191 Gif sur Yvette, France*
[2] *Unit Mixte CNRS/Saint-Gobain, Surface du Verre et Interfaces, 39 Quai Lucien Lefranc, 93303 Aubervilliers cedex, France*
[3] *Facultad de Ingeniera Mecnica y Elctrica, Universidad Autnoma de Nuevo Len, Ave. Universidad, S/N, Ciudad Universitaria, C.P. 66450, San Nicols de los Garza, NL, Mexico*

Dynamic fracture experiments were performed in PMMA over a wide range of velocities and reveal that the fracture energy exhibits an abrupt 4-folds increase from its value at crack initiation at a well-defined critical velocity, below the one associated to the onset of micro-branching instability. This transition is associated with the appearance of conics patterns on fracture surfaces that, in many materials, are the signature of damage spreading through the nucleation and growth of micro-cracks. These results suggest a nominally brittle to quasi-brittle transition in the dynamic fracture of amorphous materials the implications of which are discussed.

PACS numbers: 46.50.+a, 62.20.M-, 78.55.Qr

Dynamic fracture drives catastrophic material failures. Over the last century, a coherent theoretical framework, the so-called Linear Elastic Fracture Mechanics (LEFM) has developed and provides a quantitative description of the motion of a single smooth crack in a linear elastic material [1]. LEFM assumes that all the mechanical energy released during fracturing is dissipated at the crack tip. Defining the fracture energy Γ as the energy needed to create two crack surfaces of a unit area, the instantaneous crack growth velocity v is then selected by the balance between the energy flux and the dissipation rate Γv. This yields [1]:

$$\Gamma \simeq (1 - v/c_R)\, K^2(c)/E, \qquad (1)$$

where c_R and E are the Rayleigh wave speed and the Young modulus of the material, respectively, and $K(c)$ is the Stress Intensity Factor (SIF) for a quasi-static crack of length c. K depends only on the applied loading and specimen geometry, and characterizes entirely the stress field in the vicinity of the crack front.

Equation (1) describes quantitatively the experimental results for dynamic brittle fracture at slow crack velocities [2]. However, large discrepancies are observed in brittle amorphous materials at high velocities [3, 4, 5, 6]. In particular (i) the measured maximum crack speeds lie in the range $0.5 - 0.6c_R$, i.e. far smaller than the limiting speed c_R predicted by Eq. (1) and (ii) fracture surfaces becomes rough at high velocities (see [3, 4] for reviews). It has been argued [7] that experiments start to depart from theory above a critical $v_b \simeq 0.4c_R$ associated to the onset of micro-branching instabilities [8]: for $v > v_b$ the crack motion becomes a multi-cracks state. This translates into (i) a dramatic increase of the fracture energy Γ at v_b, due to the increasing number of micro-branches propagating simultaneously and (ii) a non-univocal relation between Γ and v [7]. The micro-branching instability hence yielded many recent theoretical efforts [9]. However, a number of puzzling observations remain at smaller velocities. In particular, even for velocities much lower than v_b, (i) the measured dynamic fracture energy is generally much higher than that at crack initiation [7, 10, 11, 12] and (ii) fracture surfaces are found to be corrugated over length scales much larger than the microstructure scale ("mist" patterns) [13].

In this letter, we report dynamic fracture experiments in polymethylmethacrylate (PMMA), the archetype of brittle amorphous materials, designed to unravel the primary cause of these last discrepancies. We show that dynamic fracture energy exhibits an abrupt 4-folds increase from its value at crack initiation at a well-defined critical velocity v_a well below v_b. This increase coincides with the appearance of a new dissipation mechanism adding to the mere opening of smooth crack surfaces that is described in LEFM. This mechanism is clearly identified to be damage spreading through the nucleation and growth of micro-cracks the signature of which is the presence of conic patterns on post-mortem fracture surfaces. Consequences of this nominally brittle to quasi-brittle transition in dynamic fracture are finally discussed.

Dynamic cracks are driven in PMMA with measured Young modulus and Poisson ratio of $E = 2.8 \pm 0.2$ GPa and $\nu = 0.36$, which yields $c_R = 880 \pm 30$ m.s^{-1}. Its fracture energy at the onset of crack propagation was determined to be $G_c = 0.42 \pm 0.07$ kJ.m^{-2}. Specimen are prepared from $140 \times 125 \times 15$ mm^3 parallelepipeds in the x (propagation), y (loading) and z (thickness) directions by cutting a 25×25 mm^2 rectangle from the middle of one of the 125×15 mm^2 edges and then cutting a 10 mm groove deeper into the specimen (Fig. 1, bottom inset). Two steel jaws equipped with rollers are placed on both sides of the cut-out rectangle and a steel wedge (semi-angle 15°) is pushed between them at constant velocity 38 μm.s^{-1} up to crack initiation. In this so-called wedge splitting geometry, the SIF K decreases with the crack length c. To increase its value at crack initiation, and therefore the initial crack velocity, a circular hole with a

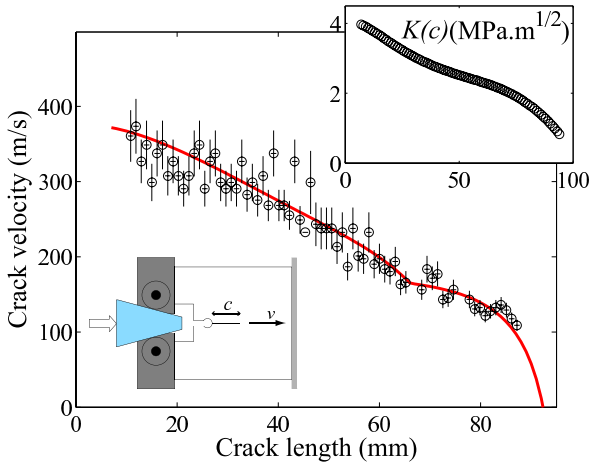

FIG. 1: (color online). Measured crack velocity v as a function of crack length c in a typical experiment ($U_0 = 2.6$ J). The vertical lines are error bars. The thick red line is the curve $v(c)$ predicted using Eq. (1) and assuming that the fracture energy is given by Eqs. (2). Top inset: Calculated quasi-static **SIF** K as a function of c. Bottom inset: Schematics of the Wedge-Splitting test.

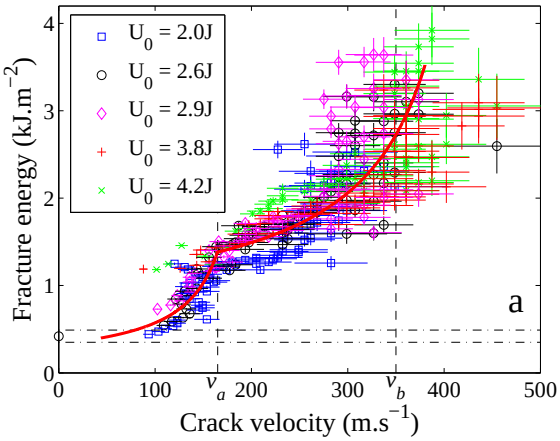

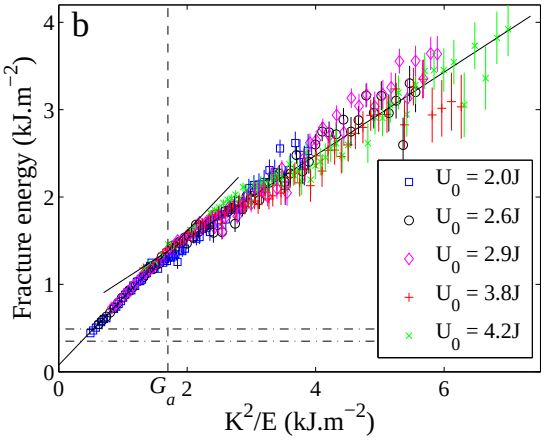

FIG. 2: (color online). (a) Fracture energy Γ as a function of crack velocity v for five different experiments with different stored mechanical energies U_0 at crack initiation. The two vertical dashed lines correspond to $v_a = 0.19c_R$ and $v_b = 0.4c_R$. The two horizontal dashed lines indicate the confidence interval for the measured fracture energy G_c at crack initiation. The thick red line represents the curve $\Gamma(v)$ predicted using Eq. (1) and assuming that the fracture energy is related to K by Eqs. (2). (b) Γ as a function of $K^2(c)/E$ (dimension of a surface energy) for the same experiments. The vertical dashed line corresponds to a crossover between two linear regimes at $K^2(c)/E = G_a \simeq 4.0G_c$. Each black line is a linear fit of the data for one out of the two regimes.

radius ranging between 2 and 8 mm is drilled at the tip of the groove to tune the stored mechanical energy U_0. Dynamic crack growth with instantaneous velocities ranging from 75 m.s^{-1} to 500 m.s^{-1} and stable trajectories are obtained. The location $c(t)$ of the crack front is measured during each experiment (40 μm and 0.1 μs resolutions) using a modified version of the potential drop technique: A series of 90 parallel conductive lines (2.4 nm-thick Cr layer covered with 23 nm-thick Au layer), 500 μm-wide with an x-period of 1 mm are deposited on one of the x-y surfaces of the specimen, connected in parallel and alimented with a voltage source. As the crack propagates, the conductive lines are cut at successive times, these events being detected with an oscilloscope. The instantaneous crack velocity $v(c)$ is computed from $c(t)$, and the instantaneous SIF $K(c)$ is calculated using 2D finite element calculations (Castem 2007) assuming plane stress conditions and constant a constant wedge position as boundary condition.

Values for the fracture energy Γ are obtained directly from Eq. (1) by combining the v measurements and the K calculations. Typical $v(c)$ and $K(c)$ curves are shown in Fig. 1. The variations of Γ with v (Fig. 2(a)) are found to be the same in various experiments performed with various stored mechanical energy U_0 at crack initiation. This curve provides evidence for three regimes, separated by two critical velocities. For slow crack velocities, Γ remains of the order of G_c as expected in LEFM. Then, as v reaches the first critical velocity $v_a \simeq 165 m.s^{-1} = 0.19c_R$, Γ increases abruptly to a value about 3 times larger than G_c. Beyond v_a, Γ increases slowly with v up to the second critical velocity, $v_b = 0.4c_R \simeq 350$ m.s^{-1}, above which Γ diverges again with v. The second critical velocity corresponds to the onset of the micro-branching instability, widely discussed in the literature [7, 8], whereas the first one, v_a, is reported here for the first time. The high slope of $\Gamma(v)$ around v_a provides a direct interpretation for the repeated observation of cracks that span a large range of Γ but propagate at a nearly constant velocity of about $0.2c_R$ (see *e.g.* refs. [14, 15]).

Provided that the equation of motion (Eq. (1)) is valid,

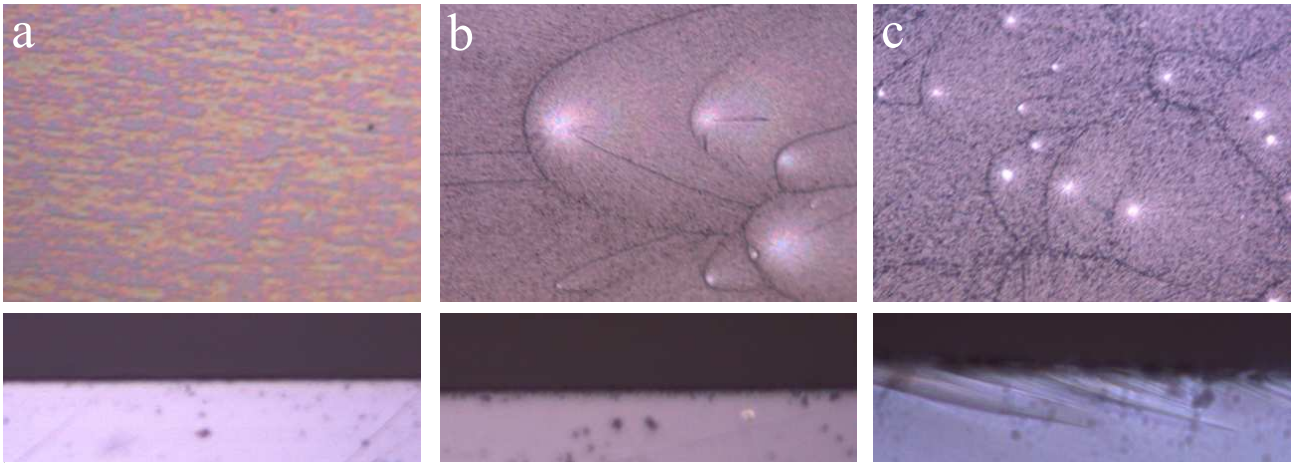

FIG. 3: Microscope images (×10) taken at (a) $v = 120 \pm 20$ m.s^{-1}, $K^2/E = 1$ kJ.m^{-2} (b) $v = 260 \pm 30$ m.s^{-1}, $K^2/E = 2$ kJ.m^{-2} (c) $v = 650 \pm 100$ m.s^{-1} ($K^2/E = 7$ kJ.m^{-2}). Top line : fracture surfaces (0.5×0.7 mm^2 field of view). Bottom line : sample sides (0.25×0.7 mm^2 field of view). Crack propagation is from left to right.

with Γ related univocally to v, an univocal relation between Γ and K is also expected. All the curves $\Gamma(K)$ for the various experiments do indeed collapse very well (Fig. 2(b)). The fracture energy is found to increase linearly with K^2/E, and the transition observed at v_a translates into a significant decrease in the slope at a critical value $G_a \simeq 1.7$ kJ/m^2 $\simeq 4.0 G_c$ associated with v_a. Γ can hence be described by:

$$\begin{array}{l} \Gamma = aK^2/E + \alpha \quad , K^2/E \leq G_a \\ \Gamma = bK^2/E + \beta \quad , K^2/E \geq G_a. \end{array} \qquad (2)$$

By fitting the curves of Fig. 2(b) we find $a = 0.77 \pm 0.02$, $\alpha = 0.08 \pm 0.03$ kJ/m^2, $b = 0.48 \pm 0.01$ and $\beta = 0.57 \pm 0.02$ kJ/m^2. No signature of the micro-branching instability is detectable in the curve $\Gamma(K)$, while a breakdown in the data collapse is observed in the curve $\Gamma(v)$ above v_b. This is likely due to the fact that the equation of motion (Eq. (1)) does not hold above v_b, meaning that in this range the curves $\Gamma(v)$ and $\Gamma(K)$ are no longer equivalent.

From the idealized curve $\Gamma(K)$ (Eqs. (2)) and the equation of motion (Eq. (1)), all the curves $v(c)$ observed experimentally can be reconstructed fairly well (thick red line in Fig. 1). Again, this reconstruction fails for $v > 380$ m.s^{-1} $\simeq v_b$ because Eq. 1 loses validity. In the same manner, the velocity dependence of the fracture energy Γ can be reconstructed (thick red line in Fig. 2(a)) from both the equation of motion and $\Gamma(K)$.

The post-mortem fracture surfaces shed light on the nature of the new transition at $v = v_a$ (resp. $K^2/E = G_a$) on the curves $\Gamma(v)$ (resp. $\Gamma(K)$). Fig. 3 shows the surface morphology for increasing crack velocity. For $v < v_a$, the fracture surfaces remain smooth at the optical scale (Fig. 3(a), top), but above this threshold, conic marks are observed (Figs. 3(b) and 3(c), top). They do not leave any visible print on the sides of the specimens (Fig. 3(b), bottom), contrary to the micro-branches that start to develop for $v \geq v_b$ (Fig. 3(c), bottom).

Similar conic marks were reported in the fracture of many other amorphous brittle materials (see [4, 13] and references therein), including polymer glasses, silica glasses and polycrystals. Their formation is thought to arise from inherent toughness fluctuations at the microstructure scale due to material heterogeneities randomly distributed throughout the material [15, 16]. The enhanced stress field in the vicinity of the main crack front activates some of the low toughness zones (nucleation centers) and triggers the initiation of secondary penny-shaped micro-cracks ahead of the crack front. Each micro-crack grows radially under the stress associated with the main crack along a plane different from it. When two cracks intersect in space and time, the ligament separating them breaks up, leaving a visible conic marking on the post-mortem fracture surface.

In this simple scenario, the distance between the conic's focus and apex is set by the distance d_n between the triggering main crack front and the nucleation center at the onset of micro-cracking. In regions where micro-cracks are observed but micro-branches are not, d_n is found to be in the range $10 - 100$ μm, which is consistent with the above description. A nucleation center in the material will initiate a micro-crack when submitted to a stress of the order of the intrinsic strength σ^* of the material ($\sigma^* \simeq 500$ MPa in PMMA [17]). Due to the square root stress singularity at the crack tip, the stress at a distance d_n from the crack front is $\simeq K/\sqrt{d_n}$. Hence we recover the observed range $d_n \simeq (K/\sigma^*)^2 \simeq 10 - 60$ μm for K in the range $2 - 4$ MPa explored in the experiments.

Fig. 4 shows the surface density of conic marks ρ as a function of crack velocity v. Below v_a, no conic mark

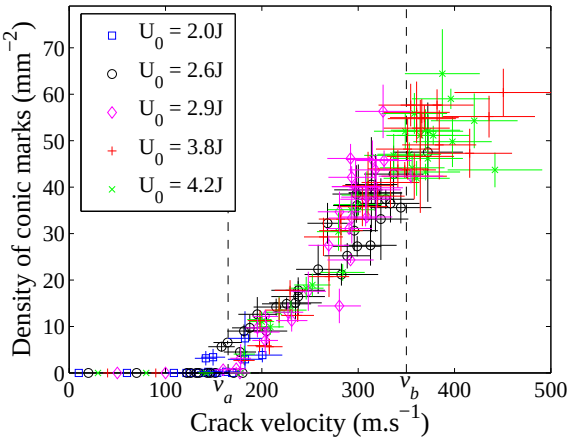

FIG. 4: (color online). Surface density ρ of conic marks as a function of crack velocity for all experiments shown in Fig. 2.

is observed at $\times 10$ magnification. Above v_a, ρ increases almost linearly with $v - v_a$. The exact correspondence between the critical velocity v_a at which Γ exhibits an abrupt increase and the velocity at which conic marks appear on the fracture surfaces strongly suggests that both phenomena are associated with the same transition. The nucleation and growth of micro-cracks can therefore be identified as the dissipation mechanism that starts at v_a. This damage process is generic in brittle materials and is relevant for an even wider range of materials than those that exhibit conic marks, *e.g.* granite [18].

Our results also shed new light on the standard "mirror-mist" transition in fractography. The latter refers to the change in morphology of the fracture surfaces as the crack accelerates. Slow cracks leave optically flat ("mirror") surfaces whereas faster cracks produce rougher ("mist") surfaces that scatter light [13]. Such a definition emphasizes changes in roughness at an arbitrary length scale, the wavelength of light, with no mechanical relevance. The origins of this roughening remain currently highly debated [19]. In the present experiments, the "mirror-mist" transition corresponds exactly to the abrupt increase in fracture energy at v_a. We thus propose that the "mirror-mist" transition be defined coherently for all brittle amorphous materials as the energetic transition associated with the onset of micro-cracking damage, regardless of the length scale at which micro-cracks alter the fracture surfaces.

In conclusion, above a well-defined critical velocity, but well before micro-branching instabilities, crack propagation in nominally brittle materials is accompanied by damage spreading through micro-cracks, which significantly increases the dynamic fracture energy. This *nominally brittle to quasi-brittle transition* should be taken into account in future conceptual and mathematical descriptions of dynamic fracture. In this respect, Continuum Damage Mechanics (CDM) [20] initially derived for "real" quasi-brittle materials like ceramics or concrete may be relevant to describe fast crack growth in nominally brittle materials. We finally emphasize that the nucleation and subsequent growth of a given micro-crack are fully set by two experimentally accessible geometric parameters, namely the position of its nucleation center and its nucleation distance. Work in progress aims at characterizing and understanding the statistical distribution of both parameters.

We thank P. Viel and M. Laurent (SPCSI) for gold deposits, T. Bernard (SPCSI) for technical support, K. Ravi-Chandar (Univ. of Texas, Austin) for fruitful discussions and P. Meakin (INL/PGP) for a careful reading of the manuscript. We acknowledge funding from French ANR through Grant No. ANR-05-JCJC-0088 and from Mexican CONACYT through Grant No. 190091.

* Present address: PGP, University of Oslo, Oslo, Norway; Electronic address: julien.scheibert@fys.uio.no
† Present address: LARMAUR, University of Rennes 1, Rennes, France

[1] L. Freund, *Dynamic Fracture Mechanics* (C.U.P., 1990).
[2] H. Bergkvist, Eng. Fract. Mech. **6**, 621 (1974).
[3] J. Fineberg and M. Marder, Phys. Rep. **313**, 1 (1999).
[4] K. Ravi-Chandar, *Dynamic Fracture* (Elsevier, 2004).
[5] A. Livne, et al., Phys. Rev. Lett. **98**, 124301 (2007).
[6] A. Livne, et al., Phys. Rev. Lett. **101**, 264301 (2008).
[7] E. Sharon and J. Fineberg, Nature **397**, 333 (1999).
[8] J. Fineberg, et al., Phys. Rev. Lett. **67**, 457 (1991).
[9] M. Adda-Bedia, Phys. Rev. Lett. **93**, 185502 (2004); H. Henry and H. Levine, Phys. Rev. Lett. **93**, 105504 (2004); E. Bouchbinder, et al., Phys. Rev. E **71**, 056118 (2005); H. Henry, EPL **83**, 16004 (2008).
[10] J. F. Kalthoff, et al., Int. J. Fract. **12**, 317 (1976).
[11] A. J. Rosakis, et al., J. Mech. Phys. Solids **32**, 443 (1984).
[12] A. Bertram and J. F. Kalthoff, Materialprfung **45**, 100 (2003).
[13] D. Hull, *Fractography* (C.U.P., 1999).
[14] K. Ravi-Chandar and W. G. Knauss, Int. J. Fract. **26**, 141 (1984).
[15] K. Ravi-Chandar and B. Yang, J. Mech. Phys. Solids **45**, 535 (1997).
[16] A. Smekal, Osterr. Ing. Arch. **7**, 49 (1953).
[17] C. A. Buckley, et al., J. Appl. Polym. Sci. **44**, 1321 (1992).
[18] D. E. Moore and D. A. Lockner, J. Struct. Geol. **17**, 95 (1995).
[19] T. Cramer, et al., Phys. Rev. Lett. **85**, 788 (2000); D. Bonamy and K. Ravi-Chandar, Phys. Rev. Lett. **91**, 235502 (2003); M. J. Buehler and H. Gao, Nature **439**, 307 (2006); G. Wang, et al., Phys. Rev. Lett. **98**, 235501 (2007); A. Rabinovitch and D. Bahat, Phys. Rev. E **78**, 067102 (2008).
[20] L. M. Kadanov, *Introduction to Continuum Damage Mechanics* (Martinus Nijhoff Publishers, 1986).